Study on the Pull–In Instability of Gold Micro-Switches Using Variable Length Scale Parameter

M. Fathalilou[1,*], M. Sadeghi[2], G. Rezazadeh[1], M. Jalilpour[1], A. Naghilou[1], S. Ahouighazvin[1]

[1]*Department of Mechanical Engineering, Khoy Branch, Islamic Azad University, Khoy, Iran*
[2]*Department of Mechanical Engineering, University of Tabriz, Tabriz, Iran*

ABSTRACT

In this paper, the size dependent behavior of the gold micro-switches has been studied. This behavior becomes noticeable for a structure when the characteristic size such as thickness or diameter is close to its internal length-scale parameter. The size dependent effect is insignificant for the high ratio of the characteristic size to the length-scale parameter, which is the case of the silicon base micro-beams. On the other hand, in some types of micro-beams like gold base, the size dependent effect cannot be overlooked. In such cases, ignoring this behavior in modeling will lead to incorrect results. Some previous researchers have applied classic beam theory on their models and imposed a considerable hypothetical value of residual stress to match their theoretical results with the experimental ones. In this study, by obtaining the equilibrium positions or fixed points of the gold micro-beam, a considerable difference between the obtained fixed points using classic beam theory and modified couple stress theory has been shown. In addition, it has been shown that the calculated pull-in voltages using modified couple stress theory are much closer to the experimental results than those obtained by classic beam theory. Finally, it has been shown that considering a unique value of length scale parameter, especially for the smallest values of the beam thicknesses, may leads to inaccurate results and variable length scale parameter should be considered.

© 2011 IAU, Arak Branch. All rights reserved.

Keywords: MEMS; Gold micro-switch; Couple stress theory; Length-scale parameter; Pull-in voltage

1 INTRODUCTION

IN recent years, gold thin films have been increasingly used in microelectronics and micro-electro-mechanical systems (MEMS) [1]. In most cases, gold has been used due to its exceptional combination of oxidation resistance and electrical conductivity, stimulating applications in multilayered thin films and MEMS micro-switches [2-4]. In such cases, the thicknesses of gold beams are typically of the order of microns and sub-microns [5-9]. In such applications, many researches show that the materials have strong size dependence in deformation behavior [10-14]. Size-dependent behavior is an inherent property of materials, which appears for a beam when the characteristic size such as thickness or diameter is close to the internal length-scale parameter of materials [14]. While the conventional theories of mechanics are incapable of describing size effects due to the lack of the material length-scale parameter, the couple stress theory (CST) is able to handle the size dependence problem.

On the other hand, the classical CST is a higher order continuum theory that contains two higher-order material length-scale parameters, which appear in addition to the two classical Lame's constants [15]. Some previous

_____

* Corresponding author. Tel.: +98 914 363 6714.

E-mail address: m.fathalilou@tabrizu.ac.ir (M. Fathalilou).

researchers have studied the static and dynamic problems based on the CST [16, 17]. To reduce the difficulties of determining length-scale parameters of materials by experiments, Yang et al. [18] introduced the modified couple stress theory (MCST), in which the couple stress tensor is symmetric and only one internal material length-scale parameter is involved. Utilizing the MCST, Park and Gao [19] studied the static response of an Euler–Bernoulli beam and interpreted the outcomes of an epoxy polymeric beam bending test. Recently, Shengli et al. [14] derived the governing equation, initial and boundary conditions of an *Euler–Bernoulli* beam using the MCST and Hamilton principle. As they reported, the stiffness of beams is size-dependent. In addition, the difference between the stiffness obtained by the classical beam theory (CBT) and those predicted by the MCST is significant when the beam characteristic size is comparable to the internal material length-scale parameter.

For bulk gold, Zong et al. [20] have shown that the length scale parameter has a unique value, whereas Cao et al. [4] have shown that the material length scale parameter increases with increasing the Au film thickness. In electrostatically actuated micro-switches, the micro-structure is balanced between electrostatic attractive force and mechanical (elastic) restoring force, both of which are increased when the electrostatic voltage increases. When the voltage reaches the critical value, pull-in instability happens. Pull-in is the point at which the elastic restoring force can no longer balance the electrostatic force. Further, increasing the voltage will cause the structure to have dramatic displacement jump, which causes structure collapse. Pull-in instability is a snap-through like behavior and it is saddle-node bifurcation type of instability [21]. In some devices such as micro-mirrors and micro-resonators, the designer avoids this instability to achieve stable motions, while in switching applications the designer exploits this effect to optimize device's performance. In practice, pull-in instability of micro-switches is suitable for changing the state of an electric circuit from open to close or vice versa [22].

Considering gradual application of the DC voltage [5-8], the pull-in phenomena is predicted based upon static analysis in a number of previous studies. However, some other researches introduced a dynamic pull-in voltage [23, 24] which is defined as a step DC voltage, and when is applied suddenly, leads to the instability of the system [23]. It should be mentioned that the scenario of instability in the case of step voltage application is different from its gradual application. When the applied DC voltage approaches static pull-in voltage, the system tends to an unstable equilibrium position by undergoing to a saddle node bifurcation, which is seen in the static application of voltage. It is a local stationary bifurcation which can be analyzed based upon locally defined eigen-values. On the other hand, periodic orbits type phenomena that cannot be analyzed via locally defined eigen-values are called global bifurcations in which the dynamic pull-in is one of them.

In MEMS technology, the micro-beams can be made of various materials such as silicon [5-8], gold [25, 26], nickel [27, 28], etc. Silicon and Silicon (Si)-based materials are the most commonly used materials in MEMS devices such as actuators, sensors and so forth. The length-scale parameter of silicon is in order of Pico-meter*,* which makes no considerable difference between CBT and higher order theories in a micro-scale system [29]. On the other hand, some materials such as gold, especially used in RF MEMS, have a length-scale parameter of order of μm and the difference between CBT and higher order theories, especially in lower beam characteristic size, is expected to be significant [30]. In spite of this fact, most of previous studies used CBT to predict the pull-in voltage of micro-beams [25-27], which caused to introduce a considerable values of hypothetical residual stresses to match their model and experimental results.

Here, it is shown that using CBT may leads to incorrect results in the modeling and designing of a number of MEMS devices and higher order mechanical theories should be applied. Some previous studies have applied the CBT in their models and introduced a considerable hypothetical value of residual stress to match their experimental and incorrect theoretical results where an effect of residual stresses is so lower than their hypothesis. Using CBT and MCST, mechanical behavior of electrostatically actuated micro-beams is modeled in this paper. Governing static and dynamic equations are solved using Galerkin based SSLM and reduced order model, respectively. The pull-in voltage of proposed silicon beam is calculated and compared to the previous theoretical and experimental results. The obtained pull-in voltages based on proposed theories are subsequently compared for the gold micro-beam and the difference between results are shown. Moreover, it is shown that the variability of the length scale parameter must be considered in investigating the mechanical behavior and pull-in instability of the gold microbeams with sub-micron thickness.

2   NONLINEAR ELECTROMECHANICAL COUPLED MODEL

Fig. 1 shows a schematic view of an electrostatically actuated micro-switch. The device consists of a fixed-fixed micro-beam, suspended over a dielectric film deposited on top of the center conductor and fixed both ends to the
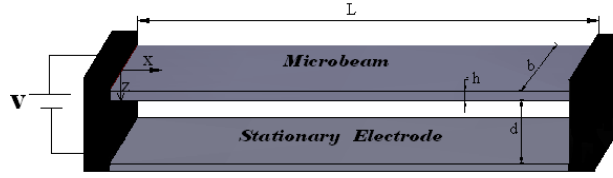
Fig. 1
A schematic view of an electrostatically actuated micro-switch.

ground conductor. When a voltage is applied between the upper and lower electrodes, the upper deformable beam is pulled down due to the electrical force.

According to the modified couple stress theory of Yang et al, the governing equation of motion for the micro-beam and corresponding boundary conditions at $x = 0$ and $x = L$ are defined as [18]:

$$\rho A \frac{\partial^2 w}{\partial t^2} + (\overline{E}I + GAl^2) \frac{\partial^4 w}{\partial x^4} = q(x,t) \tag{1}$$

$$w(0,t) = w(L,t) = 0 \ , \qquad \frac{\partial w}{\partial x}(0,t) = \frac{\partial w}{\partial x}(L,t) \tag{2}$$

where $\overline{E}$ is dependent on the beam width, b and film thickness, h. A beam is considered wide when $b \geq 5h$. Wide beams exhibit plane-strain conditions, and therefore, $\overline{E}$ becomes the plate modulus $E/(1-\upsilon^2)$, where E and υ are the Young's modulus and Poisson's ratio, respectively. A beam is considered narrow when $b < 5h$. In this case, $\overline{E}$ simply becomes the Young's modulus E. I is the effective moment of inertia of the cross-section and is $bh^3/12$ which is wide relative to thickness and width. G and l are shear modulus and length scale parameter of the beam material, respectively. Also, ρ and A are density and cross section area of the beam, respectively. It can clearly be seen in Eq. (1) the bending rigidity of the beam concerns with two parts, a part associated with EI as bending rigidity of the classical theory, another part associated with GAl^2 relates to the modified couple stress theory.

The presence of l enables the incorporation of the material micro-structural features in the new model and renders it possible to explain the size effect. Clearly, when the micro-structural effect is suppressed by letting $l = 0$, the new model defined by Eq. (1) will reduce to the classical *Euler–Bernoulli* beam model:

$$\overline{E}I \frac{\partial^4 w}{\partial x^4} + \rho bh \frac{\partial^2 w}{\partial t^2} = q(x,t) \tag{3}$$

In electrostatically actuated micro-beams, the external lateral distributed force per unit length $q(x,t)$ is written as [8, 31]:

$$q(x,t) = \frac{\varepsilon b V^2(t)}{2(d-w)^2} \tag{4}$$

where $V(t)$ is the applied voltage between the stationary and movable electrodes. ε and d are the dielectric constant of the gap medium and initial gap, respectively. For convenience in analysis, Eq. (1) can be non-dimensionalized. In particular, both the transverse displacement, w and the spatial coordinate, x, are normalized by characteristic lengths of the system and the gap size and beam length, respectively, according to: $\hat{w} = w/d$ and $\hat{x} = x/L$. Time is non-dimensionalized by the classic characteristic period of the system according to: $\hat{t} = t/t^*$ with $t^* = (\rho bhL^4/EI)^{1/2}$.

Substituting these parameters into Eq. (1), the following non-dimensional equation is obtained:

$$(1+\alpha) \frac{\partial^4 \hat{w}}{\partial \hat{x}^4} + \frac{\partial^2 \hat{w}}{\partial \hat{t}^2} = \beta \left(\frac{V(t)}{1 - \hat{w}(\hat{x},\hat{t})} \right)^2 \tag{5}$$

The parameters *α,* and *β,* appeared in Eq. (5) are:

$$\alpha = \frac{GAl^2}{\overline{EI}} \quad \text{and} \quad \beta = \frac{6\varepsilon L^4}{Eh^3 d^3} \tag{6}$$

The static equation can be derived by dropping the time dependent terms from the dynamic equation of motion:

$$(1+\alpha)\frac{\partial^4 \hat{w}_s}{\partial \hat{x}^4} = \beta(\frac{V}{1-\hat{w}_s}) \tag{7}$$

3 NUMERICAL SOLUTION

Due to the nonlinearity of the derived static equation, the solution is complicated and time consuming. Direct applying the Galerkin method or finite difference method creates a set of nonlinear algebraic equation. The method used here consists of two steps. In first step, step-by-step linearization method (SSLM) is applied [8, 31] and in the second one, Galerkin method for solving the linear obtained equation is used. For using the SSLM, it is supposed that the $\hat{w}_s^k$ is the displacement of beam due to the applied voltage V^k. Therefore, by increasing the applied voltage to a new value, the displacement can be written as:

$$\hat{w}_s^{k+1} = \hat{w}_s^k + \delta\hat{w} = \hat{w}_s^k + \psi(\hat{x}) \tag{8}$$

when

$$V^{k+1} = V^k + \delta V \tag{9}$$

So, the equation of static deflection of the fixed-fixed micro-beam Eq. (7) can be rewritten at step of $k+1$ as following:

$$(1+\alpha)\frac{\partial^4 \hat{w}_s^{k+1}}{\partial \hat{x}^4} = \beta\left(\frac{V^{k+1}}{1-\hat{w}_s^{k+1}}\right) \tag{10}$$

Considering small value of δV, it is expected that the $\psi(\hat{x})$ would be small enough, hence using the calculus of variation theory and Taylor's series expansion about $\hat{w}_s^k$ in Eq. (10), and applying the truncation to its first order for suitable value of δV, it is possible to obtain desired accuracy. The linearized equation to calculate $\psi(\hat{x})$ can be expressed as:

$$(1+\alpha)\frac{\partial^4 \psi}{\partial \hat{x}^4} - 2\beta\frac{(V^k)^2}{(1-\hat{w}_s^k)^3}\psi - 2\beta\frac{V^k \delta V}{(1-\hat{w}_s^k)^2} = 0 \tag{11}$$

The obtained linear differential equation which is solved by Galerkin method $\psi(\hat{x})$ based on function spaces can be expressed as:

$$\psi(\hat{x}) = \sum_{j=1}^{\infty} a_j \varphi_j(\hat{x}) \tag{12}$$

In this paper, $\varphi_j(\hat{x})$ is selected as *j*th undamped mode shape of the straight micro-beam. The unknown $\psi(\hat{x})$ is approximated by truncating the summation series to a finite number, *n*:

$$\psi_n(\hat{x}) = \sum_{j=1}^{\infty} a_j \varphi_j(\hat{x}) \tag{13}$$

Substituting the Eq. (13) into Eq. (11), and multiplying by $\varphi_j(\hat{x})$ as a weight function in Galerkin method and then integrating the outcome from $\hat{x} = 0$ to 1 a set of linear algebraic equation is generated as:

$$\sum_{j=1}^{n} K_{ij} a_j = F_i, \qquad i = 1,...,n \tag{14}$$

where $K_{ij} = K_{ij}^m - K_{ij}^e$ and:

$$K_{ij}^m = (1+\alpha) \qquad K_{ij}^e = 2\beta \frac{(V^k)^2}{(1-\hat{w}_s^k)^3} \int_0^1 \varphi_i \varphi_j \mathrm{d}\hat{x}, \qquad F_i = 2\beta \frac{V^k \delta V}{(1-\hat{w}_s^k)^2} \int_0^1 \varphi_i \mathrm{d}\hat{x} \tag{15}$$

A Galerkin-based reduced order model can be used [31] to study the micro-beam response to a dynamic loading. Because of the non-linearity of electrostatic force and stretching terms, direct applying the reduced order model to the dynamic equation (Eq. (5)) leads to generation of *n* nonlinear coupled ordinary differential equation and consequently the solution is more complicated. To solve this difficulty, the forcing term in Eq. (5) are considered a constant term in each step of integration which takes the value of the previous step. Selecting time steps small enough, leads to accurate results. To achieve a reduced order model, $\hat{w}(\hat{x},\hat{t})$ can be approximated as:

$$\hat{w}(\hat{x},\hat{t}) = \sum_{j=1}^{n} T_j(\hat{t}) \varphi_j(\hat{x}) \tag{16}$$

By substituting Eq. (16) into Eq. (15) and multiplying by $\varphi_j(\hat{x})$ as a weight function in Galerkin method and integrating the outcome from $\hat{x} = 0$ to 1, the Galerkin based reduced order model is generated as:

$$\sum_{j=1}^{n} M_{ij} \ddot{T}(\hat{t}) + \sum_{j=1}^{n} K_{ij}^m T_{ij}(\hat{t}) = F_i \tag{17}$$

where *M* and K^m are mass and mechanical stiffness matrices, respectively. Also *F* introduces the forcing vector. The mentioned matrices and vector are given by:

$$M_{ij} = \int_0^1 \varphi_i \varphi_j \mathrm{d}\hat{x}, \qquad K_{ij}^m = (1+\alpha) \int_0^1 \varphi_i \varphi_j^{iv} \mathrm{d}\hat{x}, \qquad F_i = \int_0^1 \varphi_i F(V,\hat{w}) \mathrm{d}\hat{x} \tag{18}$$

Now, Eq. (18) can be integrated over time by various integration methods such as Runge-Kuta method where $\hat{w}(\hat{x},\hat{t})$ in each step of integration takes the value of previous step.

4   RESULTS AND DISCUSSION

In order to validate our numerical solution of the static analysis, a fixed-fixed silicon micro-beam is considered with the geometrical and material properties listed in Table 1. In Table 2 the calculated pull-in voltage is compared with previous works for the fixed-fixed micro-beam with properties of Table 1.

It is shown that the calculated pull-in voltages are in good agreement with those reported in the previous works. For validating of dynamic results with the previous works, a fixed-fixed micro-beam is considered with the specifications of the pressure sensor used by Hung and Senturia [32]: (*E*=149 Gpa, ρ=2330 kg/m³, *L*=610 μm, *b*=40
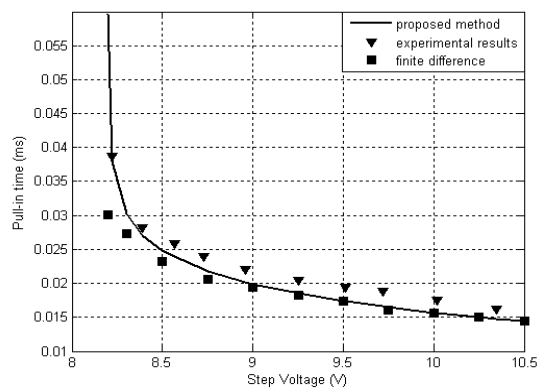
Table 1

The values of design variables [8]

Design Variable Value	Value
b	50 μm
h	3 μm
d	1 μm
E	169 GPa
ρ	2330 Kg/m^3
ε	8.85 PF/m
υ	0.06

Table 2

Comparison of the pull-in voltage for the fixed-fixed micro-beam

	Residual stress (MPa)	Our results	MEMCAD [7]	Energy model [7]
L=350	0	20.1 V	20.3 V	20.2 V
	100	35.3 V	35.8 V	35.4 V
	-25	13.8 V	13.7 V	13.8 V
L=250	0	35.9 V	40.1 V	39.5 V
	100	57.3 V	57.6 V	56.9 V
	-25	33.4 V	33.6 V	33.7 V

Fig. 2
Comparison of the pull-in time for no damping case.

μm, h=2.2 μm and d=2). Because h is given as a nominal value, it is modified to match the experimental pull-in voltage. Accordingly, thickness is obtained h=2.135 μm.

In Fig. 2 the calculated pull-in time obtained using proposed method is compared to the theoretical and experimental results of Hung and Senturia for various values of step DC voltage. The pull-in time is found by monitoring the beam response over time for a sudden rise in the displacement; at that point, the time is reported as the pull-in time [5]. As Fig. 2 illustrates, calculated results are in excellent agreement with the theoretical and experimental results. It is shown that in the no damping case for applied voltage smaller than V=8.18 V the pull in instability does not occur, so this step DC voltage can be introduced as the "dynamic pull-in voltage" for the micro-beam.

In static and dynamic validation, the micro-beams material was silicon and due to the very small value of the length-scale parameter of the silicon in comparison with its characteristic size [29], both of classic beam and couple stress theories lead to obtain the same pull-in voltages. However, what happens when the length-scale parameter have a considerable value in comparison with the material characteristic size? It is expected that the difference between the calculated pull-in voltage using the classic beam theory and the experimental pull-in voltage be so considerable. In this case, some researchers have introduced a hypothetical residual stress to their model to match their experimental and theoretical results [25-27]. For example, A. Ballestra et al. [25] for a given gold micro-beam have considered a pre-stress of 30 MPa to match their experimental and theoretical pull-in voltage. In addition, they have reported that by increasing thickness of the micro-beam, effects of the residual stresses decreases and

theoretical and experimental reports are in good agreement. To show more details, a micro-beam is considered with the geometrical parameters given by A. Ballestra et al. This gold micro-beam is introduced by properties of Table 3.

Fig. 3 illustrates the equilibrium positions or fixed points of the fixed-fixed micro-beam versus applied voltage as a control parameter. For a given applied voltage, as shown in these figure, the micro-beam has three fixed points or equilibrium positions. In addition, as shown in Fig. 3, in the state-control space, the stable and unstable branches of the fixed points, with increasing applied voltage, meet together at a saddle-node bifurcation point. The voltage corresponding to the saddle-node bifurcation point is a critical value, which is known as static pull-in voltage in the MEMS Literature. In other words, when the applied voltage equal to the static pull-in voltage there is no any basin of stable attractors on the upper side of the substrate and the micro-beam is unstable for every initial condition.

Moreover, Fig. 3 shows the saddle-node bifurcation point or pull-in voltage of the gold micro-beam. This figure represents a comparison between modified couple stress with the constant length scale parameter of l=1.12 μm, as reported by Zong et al. [20], and classic beam theories. As shown, applying modified couple stress theory shifts right the saddle-node bifurcation node and hence the calculated pull-in voltage increases. It can be shown that the difference between the two theories depends on the value of h/l. It is illustrated in Fig. 4 that by increasing the h/l ratio, the ratio of the pull-in voltage calculated by the MCST (V') to the pull-in voltage calculated by the CBT (V) approaches one, but in lower value of h/l the difference between the two theories is so considerable. In addition, in Fig. 5 the variation of the ratio of the deflection of the beam calculated by the MCST (w') to the defection calculated by the CBT (w) is shown. As illustrated in Figs. 4 and 5, considering a variable length scale parameter for the gold micro-beam, as reported by Cao et al [4] (l= 0.47,0.73 and 1.05 μm for gold film thickness of 500,1000 and 2000 nm, respectively) leads to different results from when a unique value of length scale parameter is considered. Fig. 6 shows the variation of the non-dimensional fundamental frequency of the gold micro-beam versus applied DC voltage from zero up to the pull-in voltage. As shown, applying the classic beam theory in these cases, leads to incorrect results and the modified couple stress theory must be applied.

Table 3
Geometries and material properties of the gold micro-beam [25]

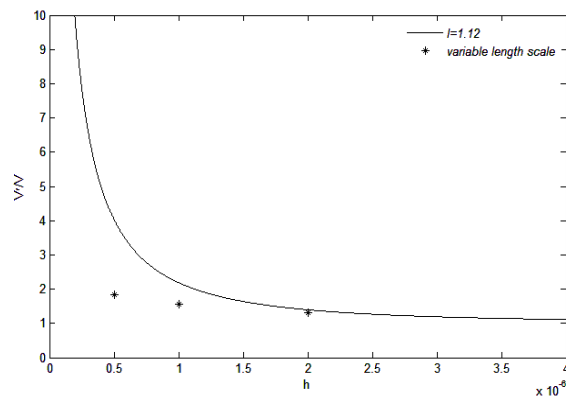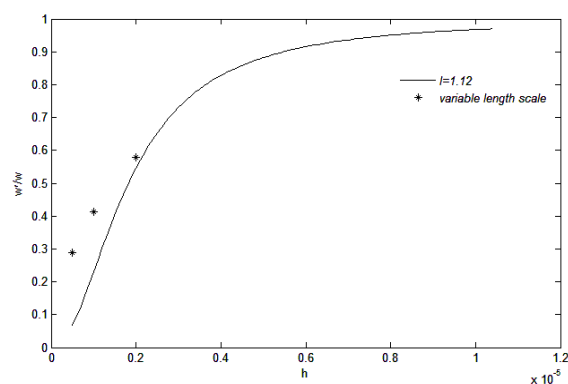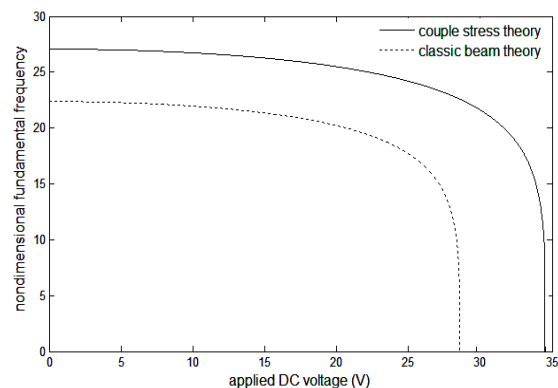| Design Variable Value	Gold
L	541.8 μm
B	32.2 μm
H	2.68 μm
D	2.83 μm
E	98.5 GPa
G	27 GPa
ρ	19300 Kg/m^3
υ	0.44
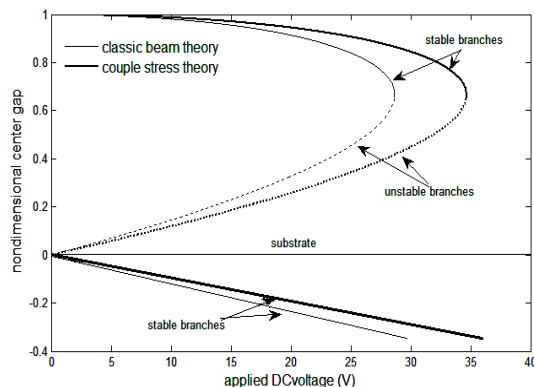
Fig. 3
Variation of the center gap of the gold micro-beam with applied DC voltage.

Fig. 4
Variation of the pull-in voltage ratio versus *h/L*.

Fig. 5
Variation of the deflection ratio versus *h/L*.

Fig. 6
Variation of the non-dimensional fundamental frequency of the gold micro-beam versus applied DC voltage (*V*=26.33V).

The dynamic pull-in phenomenon in the gold micro-switch is shown in Fig. 7. It is illustrated that by applying the classic beam theory the pull-in phenomenon occurs at $V = 26.33V$, whereas using the modified couple stress theory at this voltage, there is not a contact between the electrodes and the micro-beam is vibrating without occurring the dynamic pull-in. As the results indicate, in the gold micro-beam which has a considerable length-scale parameter in comparison with its thickness applying the classic beam theory leads to incorrect results and couple stress theory must be applied. Moreover, considering a unique length scale parameter for all beam thicknesses may not give correct results.
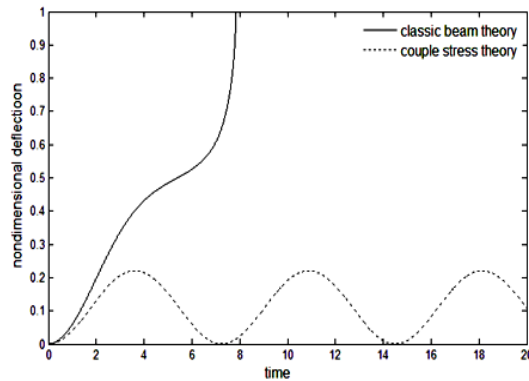
Fig.7
The response of the gold micro-beam to a step DC.

5   CONCLUSIONS

In the present study, size dependent behavior of electrostatically actuated gold micro-switches was studied. Equation of static deflection was solved using step-by-step linearization method (SSLM) and the equation of dynamic motion was solved using the Galerkin-based reduced order model. The results highlighted that in the gold micro-beam as well as other materials, having considerable length-scale parameter in comparison with their thickness, applying the classic beam theory leads to incorrect results and couple stress theory must be applied. In addition, it was illustrated that the effect of the size dependent behavior considerably grows by decreasing the ratio of the thickness to the length-scale parameter of the micro-beam. Also, it was shown that considering a unique value of length scale parameter, especially for the smallest values of the beam thicknesses, may leads to inaccurate results and variable length scale parameter should be considered. Finally, it can be concluded that the actual role of the residual stress reported in some reviewed works, is so lower than they have assumed. These obtained results can be useful for the MEMS community in the optimum design of MEMS structures.

REFERENCES

[1]   Madou M., 2002, Fundamentals of Microfabrication, CRC Press, NewYork, USA, p. 497.
[2]   Holliday R., Goodman P., 2002, Going for the gold, *IEE Review*, **48**: 15-19.
[3]   Knarr R.F., Quon R.A., 1998, Direct force measurements at the smooth gold/mica interface, *Langmuir* **14**(22): 6414-6418.
[4]   Caol Y., Nankivil D.D., Allameh S., Soboyejo W.O., 2007, Mechanical properties of au films on silicon substrates, *Materials and Manufacturing Processes* **22**: 187-194.
[5]   Younis M.I., Abdel-Rahman E.M., Nayfeh A., 2003, A reduced-order model for electrically actuated microbeam-based MEMS, *Journal of Microelectromechanical Systems* **12**(5): 672-680.
[6]   Sadeghian H., Rezazadeh G., Osterberg P.M., 2007, Application of the generalized differential quadrature method to the study of pull-in phenomena of MEMS switches, *Journal of Microelectromechanical Systems* **16** (6): 1334-1340.
[7]   Osterberg P.M., Senturia S.D., 1997, M-TEST: a test chip for MEMS material property measurement using electrostatically actuated test structures, *Journal of Microelectromechanical Systems* **6**: 107-118.
[8]   Rezazadeh G., Fathalilou M., Shabani R., 2009, Static and dynamic stabilities of a microbeam actuated by a piezoelectric voltage, *Journal of Microsystem Technologies* **15**:1785-1791.
[9]   Papargyri-Beskou S., Tsepoura K.G., Polyzos D., Beskos D.E., 2003, Bending and stability analysis of gradient elastic beams, *International Journal of solids and structures* **40**: 385-400.
[10]   Lazopoulos K.A., Lazopoulos A.K., 2010, Bending and buckling of thin strain gradient elastic beams, *European Journal of mechanics A/solids* **29**: 837-843.
[11]   Asghari M., Ahmadian M.T., Kahrobaiyan M.H., Rahaeifard M., 2010, On the size-dependent behavior of functionally graded micro-beams, *Materials and Design* **31**: 2324-2329.
[12]   Park S.K., Gao X.L., 2006, Bernoulli-Euler beam model based on a modified couple stress theory, *Journal of Micromechanics and Microengineering* **16**: 2355-2359.
[13]   Fu Y., Zhang J., 2011, Size-dependent pull-in phenomena in electrically actuated nanobeams incorporating surface energies, *Applied Mathematical Modelling* **35**: 941-951.

[14]   Shengli K., Shenjie Z., Zhifeng N., Kai W., 2009, Static and dynamic analysis of micro beams based on strain gradient elasticity theory, *Journal of Engineering Society* **47**: 487-498.

[15]   Lam D.C.C., Chong A.C.M., 1999, Indentation model and strain gradient plasticity law for glassy polymers, *Journal of Material Research* **14**: 3784-3788.

[16]   Park S.K., Gao X.L., 2006, Bernoulli-Euler beam model based on a modified couple stress theory, *Journal of Micromechanics and Microengineering* **16**(11): 2355-2359.

[17]   Shengli K., Shenjie Z., Nie Z., Wang K., 2008, The size-dependent natural frequency of Bernoulli–Euler micro-beams, *Journal of Engineering Society* **46**: 427-437.

[18]   Yang F., Chong A.C.M., Lam D.C.C., Tong P., 2002, Couple stress based strain gradient theory for elasticity, *International Journal of Solids and Structure* **39**: 2731-2743.

[19]   Park S.K., Gao X.L., 2006, Bernoulli-Euler beam model based on a modified couple stress theory, *Journal of Micromechanics and Microengineering* **16**(11): 2355-23559.

[20]   Zong Z., Soboyejo W.O., 2005, Indentation size effects in face centered cubic single crystal thin films, *Materials Science and Engineering A* **404**(1–2): 281-290.

[21]   Zhang Y., Zhao Y., 2010, Numerical and analytical study on the pull-in instability of micro- structure under electrostatic loading, *Journal of Sensors Actuators A: Physics* **127**: 366-367.

[22]   Samaali H., Najar F., Choura S., Nayfeh A., Masmoudi M., 2011, A double microbeam MEMS ohmic switch for RF-applications with low actuation voltage, *Nonlinear Dynamics* **63**: 719-734.

[23]   Nayfeh A., Younis M.I., 2005, Dynamics of MEMS resonators under superharmonic and subharmonic excitations, *Journal of Micromechanics and Microengineering* **15**: 1840-1847.

[24]   Younis M.I., Miles R., Jordy D.L., 2006, Investigation of the response of microstructures under the combined effect of mechanical shock and electrostatic forces, *Journal of Micromechanics and Microengineering* **16**: 2463-2474.

[25]   Ballestra A., Brusa E., Pasquale G., Munteanu G., Soma A., 2010, FEM modelling and experimental characterization of microbeams in presence of residual stress, *Analog Integrated Circuites Signals Process* **63**: 477-488.

[26]   Vummidia K., Khater M., Abdel-Rahman E., Nayfeh A., Raman S., 2009, Dynamic pull-in of shunt capacitive MEMS switches, *Procedia Chemistry* **1**: 622-625.

[27]   Pacheco S.P., Katehi L.P.B., Nguyen C.T.C, 2000, Design of low actuation voltage RF MEMS switch, *IEEE MTT-S Digest* **1**: 165-168.

[28]   Son S., Kim J., Kwon D., 2005, Tensile properties and fatigue crack growth in LIGA nickel MEMS structures, *Materials Science and Engineering A* **406**: 274-278.

[29]   Nix W.D., Gao H., 1998, Indentation size effects in crystalline materials: a low for strain gradient plasticity, *Journal of Mechanical and Physical Solids* **46**: 411-425.

[30]   Zong Z., Soboyejo W., 2005, Indentation size effects in face centered cubic single crystal thin films, *Materials Science and Engineering A* **404**: 281-290.

[31]   Rezazadeh G., Fathalilou M., Shabani R., Tarverdilou S., Talebian S., 2009, Dynamic characteristics and forced response of an electrostatically actuated microbeam subjected to fluid loading, *Journal of Microsystem Technologies* **15**: 1355-1363.

[32]   Hung E.S, Senturia S.D., 1999, Generating efficient dynamical models for Microelectromechanical systems from a few finite-element simulation runs, *Journal of Microelectromechanical Systems* **8**: 280-289.